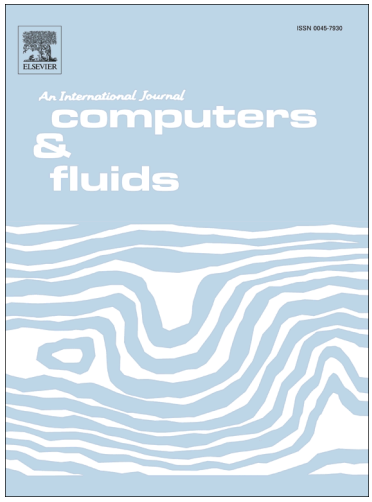

Numerical and experimental characterization of the 2D vertical average-velocity plane at the centre-profile and qualitative air entrainment inside a gully for drainage and reverse flow

J. Leandro, P. Lopes, R. Carvalho, P. Páscoa, R. Martins, M. Romagnoli

PII: S0045-7930(14)00239-4
DOI: http://dx.doi.org/10.1016/j.compfluid.2014.05.032
Reference: CAF 2582

To appear in: *Computers & Fluids*

Received Date: 16 May 2013
Revised Date: 25 April 2014
Accepted Date: 27 May 2014

Please cite this article as: Leandro, J., Lopes, P., Carvalho, R., Páscoa, P., Martins, R., Romagnoli, M., Numerical and experimental characterization of the 2D vertical average-velocity plane at the centre-profile and qualitative air entrainment inside a gully for drainage and reverse flow, *Computers & Fluids* (2014), doi: http://dx.doi.org/10.1016/j.compfluid.2014.05.032

Numerical and experimental characterization of the 2D vertical average-velocity plane at the centre-profile and qualitative air entrainment inside a gully for drainage and reverse flow

Leandro, J.[1,3,4], Lopes, P.[2], Carvalho, R.[3,4],Páscoa P.[4], Martins, R.[2] and Romagnoli, M.[5]

[1]Lecturer, Institute of Hydrology, Water Management and Environmental Techniques, Ruhr-University Bochum, 44780 Bochum, Germany, email: Jorge.Leandro@ruhr-uni-bochum.de.

[2]PhD Student, Civil Engineering Department, University of Coimbra, Coimbra, Portugal, email: pmlopes@student.dec.uc.pt and ricardo.martins@dec.uc.pt.

[3]Assistant Professor, Civil Engineering Department, University of Coimbra, Portugal, email: ritalmfc@dec.uc.pt and leandro@dec.uc.pt.

[4]IMAR-CMA Researcher, Institute of Marine Research, Marine and Environmental Research Centre, Coimbra, Portugal, email: patriciapascoaramos@gmail.com.

[5]Research Fellow, Centro Internacional Franco Argentino de Ciencias de la Información y de Sistemas /Centro Universitario Rosario de Investigaciones Hidroambientales, 27 de Febrero 210 bis, Rosario, Argentina, email: romagnoli@cifasis-conicet.gov.ar.

Abstract

Gullies are devices that connect the surface system to the sewer allowing the drainage of water during a rainfall event. During severe flooding, the sewer might become pressurized and water may gush out of the sewer onto the surface, in what is termed reverse flow. Experimental and numerical studies of gullies are rare because of the high computational time and the experimental facilities costs. In this paper we aim to characterize the average velocity inside a gully at the centre profile and discuss the qualitative air-entrainment structure for both drainage and reverse flow conditions. The experimental facility termed the Multiple-Linking-Element experiment (MLE) is located at the University of Coimbra. OpenFOAM^{TM} v.1.7.1 is used with the Large Eddy Simulation (LES) Smagorinsky model to simulate turbulence. Numerical and experimental results show reverse flow with a strong jet at the centre and an anticlockwise vortex on the left side of the gully box, and drainage flow with a large clockwise vortex located above and slightly to the left of the bottom outlet. Reverse flow shows few traces of air-entrainment, unlike drainage flow that exhibits large quantities of air-entrainment caused by a hydraulic jump formed on the surface flow.

Keywords: Computational Fluid Dynamics (CFD), Large Eddy Simulation (LES), gully, reverse flow, drainage flow

1. Introduction

Without any doubts climate change is one of the biggest challenges that communities face today while seeking to move towards more flood resilient cities [1]. One way to mitigate flooding is through the design of sewer systems in Sustainable Drainage Systems (SuDS). SuDS can be modelled through numerical hydraulic models. However flood modelling is often faced with the concern of how to model and reproduce the hydraulic behaviour of devices that connect the surface system to the sewer system such as manholes and gullies[2]. Gullies allow the water to be drained from the surface to the sewer system in "normal" conditions, or during exceptional events, they can become pressurized and water may flow in the opposite direction, which is commonly termed reverse flow. Understanding the flow through these structures in both directions is very important and shall be studied herein.

Numerical and experimental studies on gullies are rare mostly because of the difficulty in performing calibration/validation (long computational time) and cost of the experimental facilities. There are however some numerical studies on gullies using Computational Fluid Dynamic (CFD) models; these tend to have limited applicability because the gullies and manhole structures tend to vary across countries. Đjorđević et al. [3], [4] and Galambos [5] used the three-dimensional (3D) OpenFoam to model a UK gully (which is in fact a single structure manhole-gully) with a qualitative validation of the model. Carvalho et al. [6]used an In-house two dimensional vertical plane (2DV) model to do a numerical study on Portuguese gullies, and later Carvalho et al. [7] used 2D OpenFoam to model and study gullies under drainage and reverse flow. The above studies agreed on the ability of the CFD models to predict the complex air-water interfaces of the flow.

The hydraulic capacity of gullies has been experimentally studied and reported in several manuals which are normally used during design stage [8]. Gómez and Russo [9] studied in more detail the hydraulic efficiency of transverse grates and proposed some expressions to define their hydraulic efficiency. Lopes et al. [10] and Djorjdevic et al. [4] were the first to model reverse flow using CFD models. The former characterized the jet arising from the reverse flow and the latter focused on recirculation zones formed downstream of the gully. To date there are no formal studies on comparing numerical and experimental data of reverse flow or drainage flow inside the gully. To the authors knowledge, there are only three facilities that at the present time can study reverse flow in full scale; one is located at the University of Sheffield [4], the second is at the Kyoto University [11], and third is at the University of Coimbra where this study was conducted. The latter is termed the Multiple-Linking-Element experiment (MLE)[10].

The objective of this work is to numerically and experimentally characterize the 2D average velocity vertical plane inside a gully at the centre profile and discuss the qualitative air-entrainment structure for both drainage and reverse flow conditions. The experimental installation is presented in Section 2 along with the numerical model used (OpenFOAM[12]). Section 3 describes the methodology to collect the data from the experimental installation and setting up of the numerical model. Section 4 presents the calibration and validation. The numerical and experimental velocity results are presented in Section 5, followed by the discussion and comparison of the results in Section 6. Section 7 concludes the study.

2. Models

2.1 Experimental Model

The MLE experimental set-up was built inside a multipurpose flume channel at the University of Coimbra (UC) which is equipped with a SCADA system (Supervision, Control and Data Acquisition) that allows for the operation and monitoring of flow rates. The experiment is comprised of a rectangular channel, a gully and a connecting pipe (Figure 1). The channel is sloped at 1 % with 0.5 m bottom width and 0.5 m depth with 8 m long acrylic walls. The gully is an acrylic box 0.6 m long, 0.3 m depth and 0.3 m width; these are the measurements usually found in Portuguese drainage systems. The reservoir upstream of the experiment is supplied by a pumping system in a closed circuit. The channel downstream outlet is a free outfall. When modelling reverse flow, a gate is placed upstream of the gully as well as an inlet pipe of 0.08 m internal diameter that supplies the gully bottom inflow. Due to space limitations, a 90 degree bend is placed underneath the gully connection. When modelling drainage flow the gate is removed and the pipe disconnected from the gully leaving the bottom exit as a free outfall. In both cases there is no grate covering the gully. This could be the case of grate removal due to operational use [13] or projection of the grate during extreme reverse flow such as urban geysers [10].

Instantaneous velocity data set were collected using a Nortek AS® 10MHz Acoustic Doppler Velocimeter (ADV). 30 sec videos for each surcharged and drainage flow were recorded using a Panasonic DMC-FS16 camera with 14 Mega Pixels fixed on a tripod in order to visualise qualitatively the air-entrainment.

2.2 Numerical Model

The OpenFOAM™ toolbox v1.7.1 with the solver interFoam (in which the Volume-of-Fluid technique is used to track the free-surface [14]) was used to run the simulations in both directions. The algorithm PISO was chosen because it is more efficient in time-dependent calculations comparatively with SIMPLE (and its variants)[15].

Large-Eddy Simulation (LES) and Reynolds Average Simulation (RAS) are two of the usable turbulence models in OpenFOAM™ toolbox v1.7.1 with widespread applicability [16], [17] and [18]. The LES Smagorinsky turbulence model proposed by Smagorinsky [19] was adopted herein based on the authors' earlier results applying RAS (see Lopes *et al.* [20] and section **6.2**). The LES model selected in OpenFOAM contains two input parameter constants Cε and Ck which can be related with the original Smagorinsky constant Cs [21] used to calculate the eddy-viscosity coefficient. This model resolves large scales of the flow field solution with better fidelity than the Reynolds-Average Simulation (RAS) but, on the other hand, leads to higher computational cost for most hydraulic engineering problems.

Four different boundary conditions (BC) are used in the numerical model divided into two *types* in OpenFOAM terminology: *patch* and *wall*. Each boundary condition is defined in accordance with their functionality: the inlet BC allows inflow at a constant velocity definition (*patch*); the outlet BC allows outflow and the relative pressure is set to 0 (*patch*); the atmosphere BC (*patch*) sets the atmospheric

pressure (whereby the relative pressure is set to 0); the wall BC is set with the condition of no slip thus the velocity is set to 0 next to the wall (*wall*). When solving the reverse flow (Tr) the bottom and left BC are set respectively as an inlet and a wall BC, whereas when solving the drainage flow (Td) they are set as an outlet and an inlet BC, respectively (Figure 2).

3. Methodology

3.1 Experimental Methodology

In order to validate numerical model and experimentally characterize the average velocity inside the gully at the centre profile for both drainage and reverse flow conditions, first a set of flow rates was defined and secondly a spatial grid was chosen from which velocities were measured (Figure 3). The spatial grid was defined with 0.03 m spacing in order to accurately characterize the large vortices structures inside the gully box (Figure 3). The bottom of the grid is 0.05 m above the base of the gully box, which is well above the minimum (of 0.02 m) required to avoid boundary effects [22] and [23]. For reverse flow the first two columns away from the centre are displaced 0.04 from the centre and thus only 0.02 m from the next column. In total 171 and 162 points per experimental run were collected for the drainage and reverse flow tests respectively. The methodology to extract the results will now be further discussed.

In total, six tests were setup to study reverse and drainage flow experiments (**Table 1**). Three flow rates were defined for studying the reverse flow (Tr): 4, 5 and 6 l/s with Reynolds numbers (Re) between $6x10^4$ to $10x10^4$. The upper limit was constrained by the maximum flow rate allowed by the experiment. Lower values than 4 l/s would produce very small average velocities within the gully box. In case of drainage flow the following flow rates were defined as (Td): 15, 22 and 32 l/s with Reynolds numbers between $8x10^4$ and $10x10^4$. The adopted upper limit was set because the incoming flow was mostly flowing over the gully. Lower values than 15 l/s would bring large amounts of air into the gully rendering the ADV measurements useless.

The two data quality indicators normally associated with acoustic Doppler data are the correlation (COR) and the signal to noise ratio (SNR) [24]. The COR parameter reported by the instrument is a measured of the similarity of two pulse echoes being measured by the ADV. The SNR also provided by the instrument is calculated using the signal amplitude and background noise level. Both parameters should be maximized during measurements [25]. Nortek [26] suggests that SNR>5dB is required for collecting mean flow data and that SNR>15dB is necessary for collecting turbulence data. Wahl [27] claims that samples with COR<70 can provide good data, mainly when both SNR and turbulence are high. In addition, COR values as low as about 30 can be used for mean velocity measurements [28]. Spikes in the water velocity signals recorded using ADVs may be caused by phase shift ambiguities (i.e., phase shift from successive coherent acoustic return lies outside the range between −180 and 180). In addition, throughout the flow velocity measurements, aeration effects and high turbulent intensities might cause

spikes. In this work, the presence of spikes in the water velocity time series was detected by means of the phase-space thresholding method (PSTM) proposed by Goring and Nikora [29].

As mentioned earlier, instantaneous velocities were measured with an Acoustic Doppler Velocimeter (ADV) probe. The frequency and sampling period were set to 1 Hz and 180 s respectively. In the case of drainage flow the frequency was set to 25Hz because of the low signal correlation values obtained with 1Hz frequency. In any case low correlation values were still unavoidable in some points, particularly near the jet in reverse flow because of the very high turbulence readings, and in drainage flow were exceptional larger air-entrainment occurred during low flows.

3.2 Numerical Methodology

A regular non-uniform mesh with variable grid spacing from 0.01 m to 0.04 m was used for both drainage and reverse flow numerical models. Finer mesh is applied at the gully box and inlet, and coarser mesh at the channel inlet and outlet. The mesh is adapted from Martins et al. [13] and generated using blockMesh utility in OpenFOAM™ (**Figure 2**). Both reverse and drainage flow are modelled with the same grid for the sake of simplicity without retracting from the results accuracy. Indeed a qualitative comparison was done against numerical simulations with the inclusion of a 90 degree bend underneath the gully connection but did not show a clear improvement.

ParaView™ was used to extract the instantaneous velocities used to obtain the average velocity at all points in the centre spatial grid defined earlier (**Figure 3**) taken from the OpenFOAM™ output results.

4. Calibration and Validation

4.1 Steady State Check

Numerical models are sensitive to geometry, initial conditions and model parameters. In order to check that the numerical simulations indeed converged into steady state conditions from which average velocity fields could be extracted, all models were run for 20 s. The authors previous experience with similar numerical applications on the same installation showed that the last 5 s were enough to produce consistent average velocities [30] and [6].Steady state conditions were verified through the analysis of the fraction of water during the simulations. **Figures 4** and **5** show the percentage of water inside the numerical domain with time. For reverse flow the steady state is achieved after 15 s whereas for drainage flow it occurs after 5 s; in both cases the absolute errors for the last 5 s remain always below 0.5%.

4.2 LES parameters

In classical Smagorinsky model the Smagorinsky constant needs to be calibrated to fit the observed data [31]. In order to set the parameters Cε and Ck in the LES model, the 4 l/s experiment for reverse flow was selected for calibration. Several values were tested around the pre-defined OpenFOAM™ values of Cε=1.05 and Ck=0.07 (Cs=0.13). To decide on the best set of parameters, the absolute errors as the difference between the maximum velocity (Vmax) and the average velocity fields at the left (Vavl) and right (Vavr) side of the gully were calculated, and three measures of fit were estimated, namely the:

PBIAS Coefficient [32] - the Index of agreement I.d [33] and the Coefficient of determination R^2 [34].The closer the PBIAS is to 0, the more accurate is the model. The upper limit of the Index of agreement is 1.0 and indicates perfect model performance. R^2 ranges from −1.0 to 1.0; a value of 1.0 implies that a linear equation describes the relationship between experimental and numerical results perfectly. **Table 2** summarises the results obtained for the calibration. Cε=1.05 and Ck=0.03 were selected as the best parameters having in mind the measures of fit but also the computational time (e.g. when compared with the solution with Cε=1.15 and Ck=0.07, which has a smaller Vmax error but a higher PBIAS and computational time). **Table 3** summarises the results obtained for the validation. Herein is interesting to note that in terms of I.d and R^2 the calibrated run (Tr.1) and Td.1 have the best values, but not in terms of PBIAS; Td.2 has the best PBIAS, although it also shows the worst R^2. Overall the results remain good across the different tests; particularly Td.3 which has the highest discharge, whereby some disagreement in the results is often expected as the discharges differs from the calibrated value.

5. Results

5.1 Experimental

5.1.1 ADV signal quality

Figures 6 and **7** show the correlation parameter (COR) values for each experiment (Section 3.1), whereby in the legend white areas represent points where the signal was either excluded due to high turbulence readings (reverse flow) or because the probe was not fully submerged (drainage flow). Therefore white areas in the gray scale legend do not display cells with COR=100 but are rather points where the signal could not be obtained. In terms of SNR, all the recorded signals showed values larger than 5 dB.

5.1.2 Average velocities

Figures 8 and **9** show the average velocity fields measured with the ADV probe for the reverse and drainage flow using the grid defined in Figure 3. As discussed in section 3.1 the points along the centre of the jet for reverse flow were eliminated (discarded), as well as some points near the surface for drainage flow.

5.1.3 Air-entrainment

Figures 10 and **11** show images of the air-water flow randomly selected from the videos described in section 3.1., for reverse and drainage flow respectively. The pictures show a zoom of the gully box and part of the surface sloped channel. A horizontal bar which serves as structural element and a measuring tape are also visible.

5.2 Numerical

Figures 12 and **13** show the average velocity fields obtained with the numerical model for the reverse and drainage flow using the grid defined in Figure 3. Only the points retained in section 5.1.1 were plotted for comparison.

6. Discussion

6.1 Qualitative air entrainment assessment and ADV signal quality

Two distinct cases are studied in this paper; first, reverse flow, a relatively rare occurrence when sewer systems become surcharged and a second termed drainage flow, the regular or the normal expected behaviour of a gully during a rainfall event. These two cases exhibit a distinct behaviour in the MLE experimental installation. The reverse flow shows virtually no trace of air-entrainment, with some exception for occasional occurrences for 5 l/s and 6 l/s (**Figure 10**). The latter showed some air bubbles entrainment next to the upstream wall occupying at the most a length of 0.20 m away from the upstream wall inside the gully (**Figure 10 c.1)** and **c.2)**). This is in agreement with the ADV signal correlation values which are good everywhere except at the jet centre, with a local deterioration where the air-bubbles appear for 6 l/s (**Figure6c)**).

The drainage flow unlike the previous case exhibits large quantities of air-entrainment, which are mainly due to the hydraulic jump formed above the gully, particularly when it is located next to the downstream wall of the gully. For 15 and 22 l/s (**Figure 11 a)** and **b)**) the entrained air-bubbles are carried downwards in the vortex highlighted in **Figure 13**; a small percentage of the air-bubbles remain trapped inside this large vortex, while the majority is discharged through the bottom orifice. For the largest discharge rate, 32 l/s, the hydraulic jump occurs further downstream than at lower flow rates, resulting in less air-entrainment. Again the ADV signal correlation helps to identify where the large portions of air can be found; for example for 22 l/s, **Figure 7b)** clearly identifies that air is entraining from the upper right corner (with no valid readings on those points, represented by the white areas).

It should be noted that while the mechanism of air-entrainment found in drainage flow is likely to occur in full scale systems, for reverse flow that is not the case. Indeed for reverse flow there may be other sources of air-entrainment (e.g. trapped air bubbles in sewer pipes upstream) which are not considered in the MLE experimental facility. Thus for reverse flow the extrapolation of the air-entrainment assessment cannot be directly applied to real scale systems.

6.2 Average velocity profiles (numerical and experimental)

In general the numerical and experimental results show good agreement for all tests. The surcharge flow is characterized by a strong jet at the centre, almost vertical, that generates an anticlockwise vortex on the left side of the gully box with centre around the coordinates (20, 20). On the right side the velocities are very small (**Figures 8** and **12**). With the increase of flow rate the velocities increase. The centre of the vortex is in good agreement by the two models, however next to the jet location and particularly near to the top of the gully box, the numerical model tends to produce higher velocity vectors than the experimental results (**Figures 8 c)** and **12 c)**). Also the experimental model seems to show higher velocities around the vortex than the numerical model.

The drainage flow is composed of a large clockwise vortex initially located above and slightly to the left of the bottom outlet for 15 l/s and then gradually moving up with the increase of flow rate to 32 l/s. The experimental and numerical models locate the vortex centre around coordinates (22,8) and (25,15) for

15 l/s and around coordinates (25,12) and (25,15) for 32 l/s (**Figures 9** and **13**). Apart from a slight disagreement on the location of the centre, in terms of predicting the large vortex structure the agreement between the two models is very good.

In order to clearly mark the differences between the velocity fields obtained with the experimental and the numerical model, **Figures 14** and **15** superimpose the results following the numbering presented in **Figure 3** for the horizontal (Vx) and vertical velocity (Vz) components.

Except for the points next to the jet, the calibration dataset presented in **Figure 14 a)** shows an almost perfect match between the two results. **Figure 14** shows that the calibration of the LES parameters was indeed effective in obtaining a good fit. The model still shows a good performance as the flow rate increases in the reverse flow case, however compared to the calibration data set the agreement diminishes particularly in the vicinity of the jet (**Figure 14 c**)) and in several points in Vx where there are some significant velocity differences. Looking to the drainage cases the results are quite robust as a good agreement holds for the three tests, except perhaps for Vx in **Figure 15 b** where the differences become more visible. In any case the best agreement found in the drainage flow tests may arise from the large velocity gradients and higher turbulence that occur in reverse flow near the jet (**Figure 14 a)** and **c)**) which are more difficult to model numerically, whereas this is not the case for drainage flow where these gradients remain smoother across the gully box (**Figure 15**).

To some extent differences in the velocity fields between numerical and experimental results could be explained by the turbulence model not being able to fully replicate the high turbulence next to the jet in reverse flow and the localized areas where substantial air-entrainment occurs in drainage flow. Indeed it has been pointed out by some authors that LES Smagorinsky turbulence model might actually need an independent set of coefficients $C\varepsilon$ and Ck (to calculate Cs) depending on the test [35][36]. It is also well known that air plays an important role in energy dissipation [37] and thus could also affect the velocity fields within the gully. Alike other multiphase solvers, interFoam solver is not able to reproduce well the flow behaviour when the air concentration exceeds values of 15 to 20 % [38][39]. It is thus expectable that a combination of these factors may affect the simulations and to some extent explain the differences found between numerical and experimental results. Future work will be looking into methods to include air-entrainment modelling into OpenFOAM.

7. Conclusions

This paper presented numerical and experimental results of drainage and reverse flow in a gully. The average velocity inside a gully at the centre profile was characterized numerically and experimentally, and the qualitative air-entrainment structure for both drainage and reverse flow conditions were discussed based on experimental results. The turbulence closure adopted was the Large-Eddy Simulation (LES) Smagorinsky model available in OpenFOAM^{TM} toolbox v1.7.1. The average velocity results from the six different tests showed a good agreement between numerical and experimental outputs.

The MLE facility allowed the study of both drainage and reverse flow. The velocity fields were measured using an Acoustic Doppler Velocimeter (ADV) and the qualitative assessment of the air-entrainment was supported on video recordings. The ADV spike noise was removed and the signal was filtered based on correlation coefficients that measured the coherence of the signal. With the calibration of the two parameters of the LES model (in OpenFOAM), namely $C\varepsilon$ and Ck, a good agreement between numerical and experimental results was found.

The surcharge flow was characterized by a strong jet at the centre responsible for generating an anticlockwise vortex on the left side of the gully box. The location of the vortex and the velocity field in the numerical and experimental model were in good agreement. Nonetheless near the jet the numerical model values tend to be higher than the experimental values measured. The drainage flow was characterized by large clockwise vortex, clearly identified in both models. The location of the vortex, on the other hand, was slightly offset when experimental and numerical results were compared. Nonetheless in terms of the velocity values the agreement between the two models is considered good.

The qualitative air-entrainment assessment showed two distinct behaviours. The first was observed during drainage flow which showed large quantities of air-entrainment in the gully box. The main entrainment mechanism identified was the hydraulic jump that developed next to the downstream wall of the gully. A small percentage of the entrained air remained trapped inside the large vortex while the large percentage is discharged through the bottom outlet. The second was observed during reverse flow which showed virtually no traces of air-entrainment. While the former is likely to occur in real systems, the latter draws from a limitation of the current MLE experimental facility which in its current configuration cannot replicate air-entrainment originating from upstream/downstream sewer pipes.

In this study the grate covering the gully was not considered. This could be the case of grate removal due to operational use, or due to extreme reverse flow such as urban geysers. It is foreseeable that its inclusion will affect the hydraulic behaviour of the gully in both reverse and drainage flow as the grate will change the boundary conditions of the gully box. Future research is likely to include the study of reverse and drainage flow with a grate covering the gully. Furthermore we will be looking into methods to include air-entrainment modelling into OpenFOAM and to measure it experimentally in order to study the behaviour of the air-water mixture.

8. Acknowledgements

The authors would like to acknowledge financing through the FCT (“Fundação para a Ciência e Tecnologia”) and the COMPETE (“ProgramaOperacionalTemáticoFactores de Competitividade”), supported by FEDER (“Fundo Europeu de Desenvolvimento Regional”) through projects PTDC/AAC-AMB/101197/2008 and PTDC/ECM/105446/2008. The authors also thank Mr. Joaquim Cordeiro da Silva for the help provided with the experimental model.

9. References

[1] Leandro J, Santos B, Leitao JP, Siekmann T, Urich C. Towards mOre Resilient Cities (ToRC). 9th Int. Conf. Urban Drain. Model. Belgrade, Serbia, 2012, p. 1–9.

[2] Leandro J, Djordjevic S, Chen A, Savic D. The use of multiple-linking-element for connecting sewer and surface drainage networks. 32th Congr. IAHR "Harmonizing Demands Art Nat. Hydraul., 2007.

[3] Djordjević S, Chen A, Evans B, Galambos I, Leandro J, Savić DA. 1D, 2D and 3D Modelling of Urban Flooding. Water Sanit Technol Belgrade 2010;4:71–83.

[4] Djordjević S, Saul AJ, Tabor GR, Blanksby J, Galambos I, Sabtu N, et al. Experimental and numerical investigation of interactions between above and below ground drainage systems. Water Sci Technol 2013;67:535–42.

[5] Galambos I. Improved Understanding of Performance of Local Controls Linking the above and below Ground Components of Urban Flood Flows. PhD thesis, University of Exeter, UK, 2012.

[6] Carvalho R, Leandro J, Martins R, Abreu J, de Lima JLMP. 2DV numerical modelling of different flows occurring in gullies. 12th Int. Conf. Urban Drain., Porto Alegre. Brazil: 2011, p. 1–8.

[7] Carvalho RF, Leandro J, Martins R, Lopes P. Numerical study of the flow behaviour in a gully. 4th IAHR Int. Symp. Hydraul. Struct. 9-11 Febr. 2012, Porto, Port., 2012, p. 9–11.

[8] Brown, S. A., Stein, S. M., and Warner JC. Urban drainage design manual, hydraulic engineering. Circ No 22, FHA, US Dept Transp Washington, DC 1996.

[9] Gómez M, Russo B. Hydraulic Efficiency of Continuous Transverse Grates for Paved Areas. J Irrig Drain Eng 2009;135:225–30.

[10] Lopes P, Leandro J, Carvalho RF, Páscoa P, Martins R. Numerical and experimental investigation of a gully under surcharge conditions. Urban Water J 2013:1–9.

[11] Bazin J-P. Flows during floods in urban areas: influence of the detailed topography and exchanges with the sewer system,. PhD thesis, University of Lyon, 2013.

[12] Ubbink O. Numerical prediction of two fluid systems with sharp interfaces. Imperial College of Science, UK, 1997.

[13] Martins R, Leandro J, Carvalho RF De. Hydraulic behaviour of a gully under drainage conditions : numerical vs . experimental. 9th Int Conf Urban Drain Model Belgrade, Serbia 2012.

[14] Hirt, C.W. and Nichols BD. Volume of fluid (VOF) method for the dynamics of free boundaries. J Comput Phys 1981:201–25.

[15] Versteeg HK, Malalasekera W. An Introduction to Computational Fluid Dynamics - The Finite Volume Method. Longman Sci Tech 1995:75, 78 and 154.

[16] Dufresne M, Vazquez J, Terfous A, Ghenaim A, Poulet J-B. Experimental investigation and CFD modelling of flow, sedimentation, and solids separation in a combined sewer detention tank. Comput Fluids 2009;38:1042–9.

[17] Serre E, Minguez M, Pasquetti R, Guilmineau E, Deng GB, Kornhaas M, et al. On simulating the turbulent flow around the Ahmed body: A French–German collaborative evaluation of LES and DES. Comput Fluids 2013;78:10–23.

[18] Yu Y-H, Li Y. Reynolds-Averaged Navier–Stokes simulation of the heave performance of a two-body floating-point absorber wave energy system. Comput Fluids 2013;73:104–14.

[19] Smagorinsky J. General Circulation Experiments with the Primitive Equations. Weather Rev 1963;91:99–164.

[20] Lopes P, Leandro J, Carvalho R, Martins R. Hydraulic behaviour of a gully under surcharge conditions. 9th Int. Conf. Urban Drain. Model. Belgrade, Serbia, vol. Belgrade 2, 2012, p. 1–10.

[21] Peter E. Sullivan, Mcwilliams JC, Moeng. C-H. A SubGrid-Scale Model for Large-Eddy Simulation of Planetary Boundary-Layer Flows. Boundary-Layer Meteorol 1994:247–76.

[22] Precht E, Janssen F, Huettel M. Near-bottom performance of the acoustic Doppler velocimeter (ADV) - a comparative study. Aquat Ecol 2006;40:481–92.

[23] Liu M, Rajaratnam N, Zhu DZ. Evaluation of ADV measurements in bubbly two-phase flows. Proc Spec Conf 2002, Estes Park Color 2002.

[24] Rusello, P. J. A practical primer for pulse coherent instruments. Nortek Tech Note N^{o} TN-027 2009.

[25] McLelland SJ, Nicholas AP. A new method for evaluating errors in high-frequency ADV measurements. Hydrol Process 2000;14:351–66.

[26] Nortek. ADV operation manual. Nortek AS 1997.

[27] Wahl T. Analyzing ADV data using WinADV. ASCE Jt. Conf. Water Resour. Eng. Water Resour. Plan. Manag. Minneapolis, July 30–August 2, 2000, USA., 2000.

[28] Sontek. SonTek/YSI ADVField/Hydra Acoustic Doppler Velocimeter (Field). Tech Doc SonTek/YSI, San Diego, USA 2001.

[29] Goring, D.G., and Nikora VI. Despiking ADV data. J Hydraul Eng 2002;128:117–26.

[30] Martins R, Leandro J, Carvalho RF. Hydraulic behaviour of a gully under drainage conditions: numerical vs . experimental. 9th Int. Conf. Urban Drain. Model. Belgrade, Serbia, 2012, p. 1–11.

[31] Damián SM, Nigro NM. Comparison of Single Phase Laminar And Large Eddy Simulation (LES) Solvers Using The OpenFOAM Suite. Asoc Argentina Mecánica Comput 2010;XXIX:3721–40.

[32] Liew MW Van, Bingner RL, Harmel RD, Veith TL. Model evaluation guidelines for systematic quantification of accuracy in watershed simulations. Trans ASABE 2007;50:885–900.

[33] Willmott CJ. On the validation of model. Phys Geogr 1981;2:184–94.

[34] Pearson K. Mathematical Contributions to the Theory of Evolution. III. Regression, Heredity and Panmixia. Philos Trans R Soc London 1896;187:253–318.

[35] Blazek J. Computational Fluid Dynamics: Principles and Applications. 1st. Elsevier Science B.V. ISBN: 0 08 043009 0: 2001.

[36] Qian Z, Hu X, Huai W, Amador A. Numerical simulation and analysis of water flow over stepped spillways. Sci China Ser E Technol Sci 2009;52:1958–65.

[37] Lubin P, Glockner S, Kimmoun O, Branger H. Numerical study of the hydrodynamics of regular waves breaking over a sloping beach. Eur J Mech - B/Fluids 2011;30:552–64.

[38] Deshpande SS, Trujillo MF, Wu X, Chahine G. Computational and experimental characterization of a liquid jet plunging into a quiescent pool at shallow inclination. Int J Heat Fluid Flow 2012;34:1–14.

[39] Xiangju C, Xuewei C. Progress in numerical simulation of high entrained air-water two-phase flow. 3rd Int. Conf. Digit. Manuf. Autom. (ICDMA2012), (July 31 - August 2 2012, GuiLin, China Conf. Publ. Serv. - IEEE Comput. Soc., 2012, p. 626–9.

List of Figures

Fig. 15 Comparison of the numerical and experimental average velocity vector field for drainage flow for 15(a), 22(b) and 32(c) l/s.

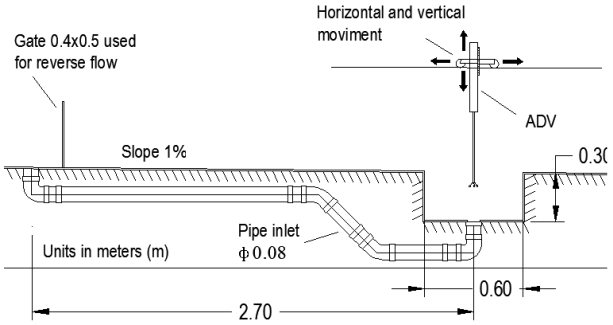

Fig. 1 Sketch of the MLE experimental Installation used for studying reverse flow in the Gully (0.6x0.3x0.3 m); for drainage flow the bottom pipe (0.08 m) is disconnected and the gate removed.

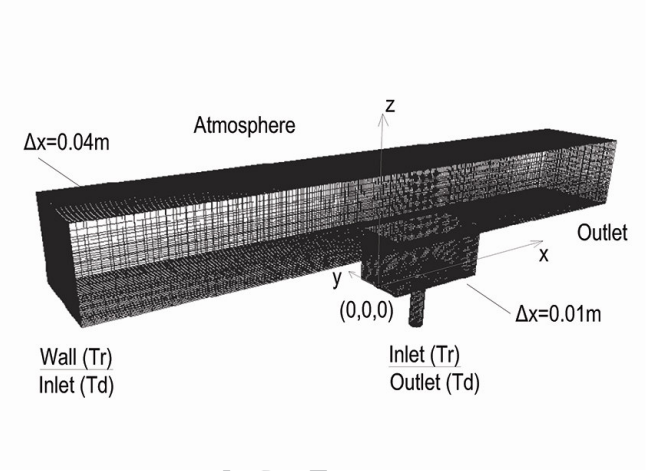

Fig. 2 3D view of the grid and boundary conditions (Wall, Inlet, Outlet and Atmosphere) used in the numerical model OpenFOAM for studying reverse flow (Tr) in the Gully; for drainage flow (Td) conditions the bottom Inlets replaced by an Outlet, and the left wall by an Inlet condition.

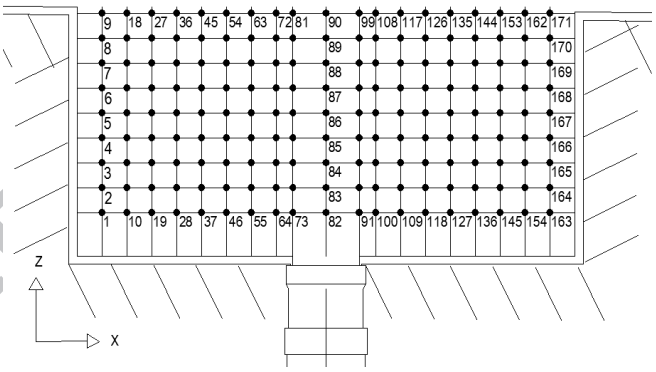

Fig. 3 2D view of the grid used with 0.03 m spacing to measure the instantaneous velocities in the experimental and numerical model for reverse flow. The two columns either side of the centre are displaced by 0.04 m from the centre and thus only 0.02 m from the next column. For drainage flow spacing between points is kept constant and equal to 0.03 m.

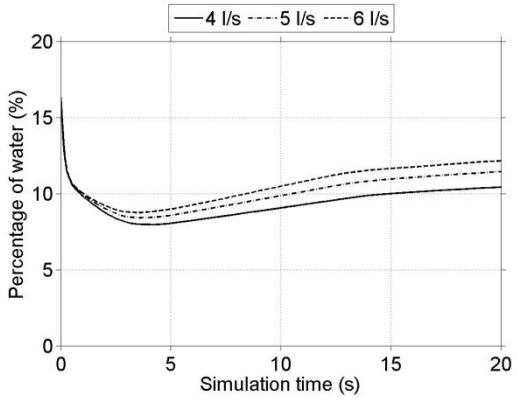

Fig. 4 Steady state convergence check for the reverse flow numerical model

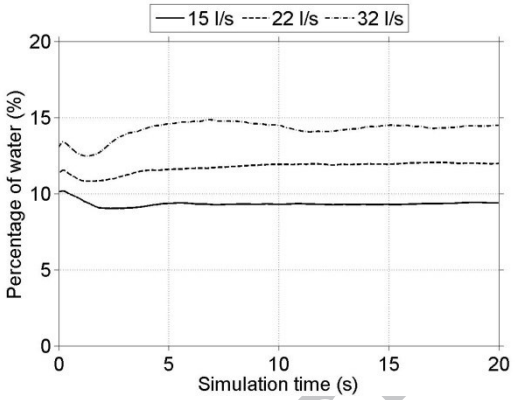

Fig. 5 Steady state convergence check for the reverse flow numerical model

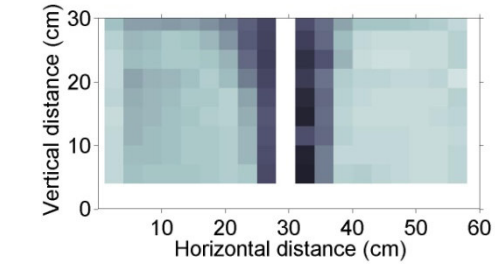

a)

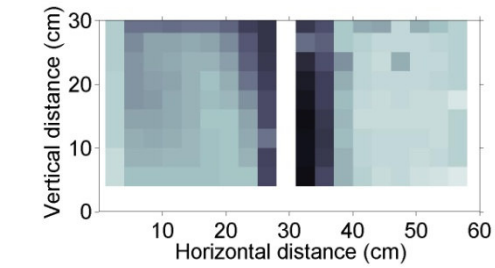

b)

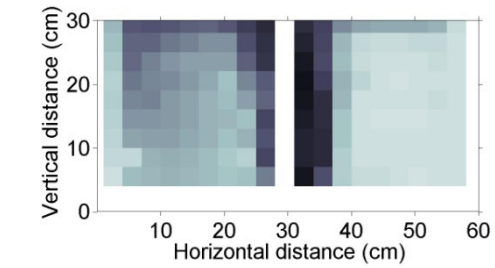

c)

Fig. 6 Spatial distribution of the ADV signal correlation coefficients (COR) in the reverse flow experimental model for 4 (a), 5 (b) and 6 (c) l/s. Note that due to the gray scale used, white areas do not have COR=100 but are rather excluded because of high turbulence readings.

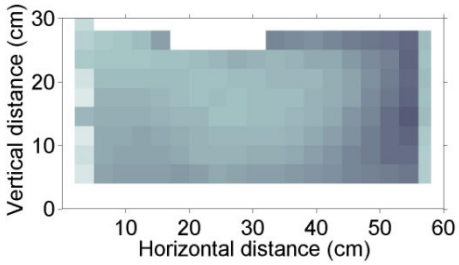

a)

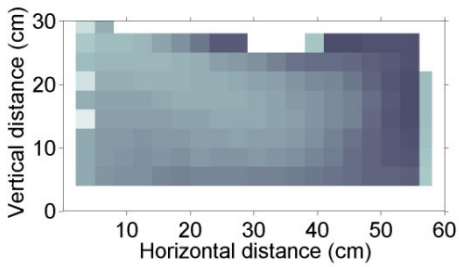

b)

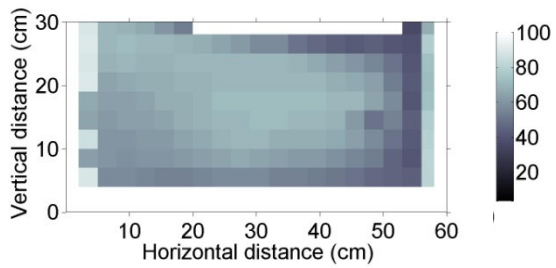

c)

Fig. 7 Spatial distribution of the ADV signal correlation coefficients (COR) in the drainage flow experimental model for 15 (a), 22 (b) and 32 (c) l/s. Note that due to the gray scale used, white areas do not have COR=100 but are rather excluded because of incomplete submersion of the probe.

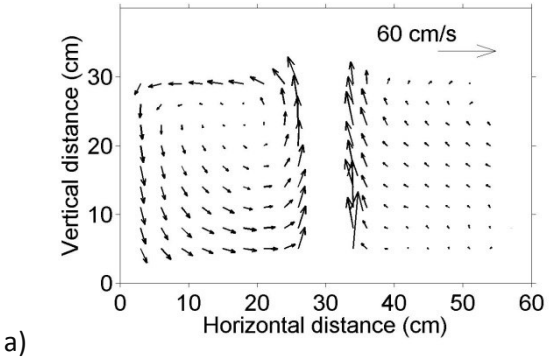

a)

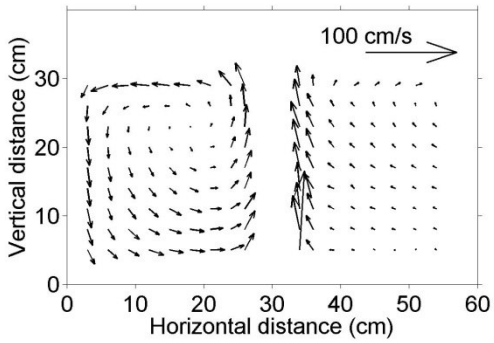

b)

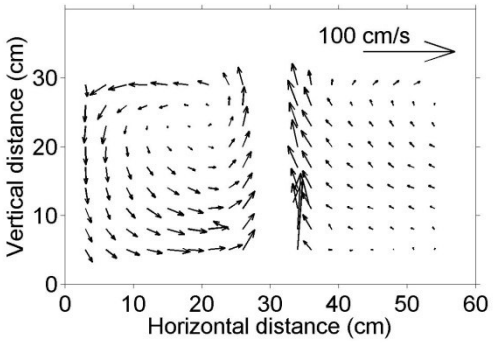

c)

Fig. 8 Average velocity vector field measured with the ADV for reverse flow for 4(a), 5(b) and 6(c) l/s.

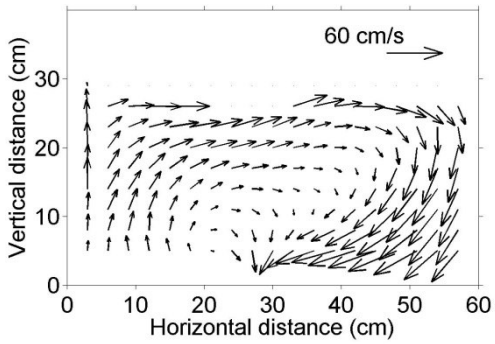

a)

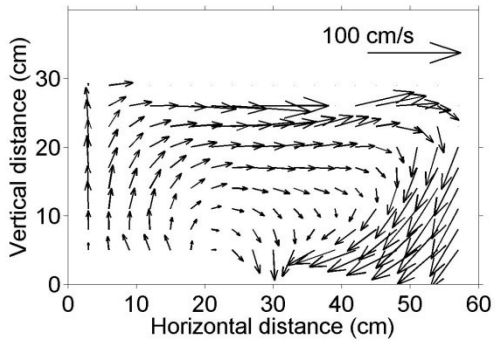

b)

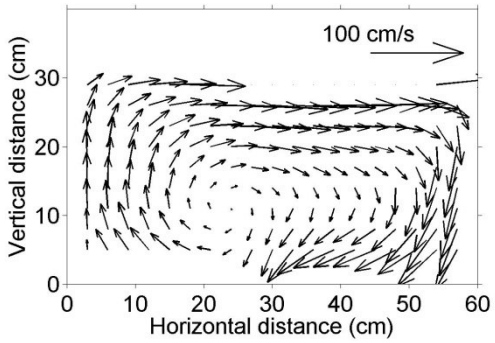

c)

Fig. 9 Average velocity vector field measured with the ADV for drainage flow for 15(a), 22(b) and 32(c) l/s.

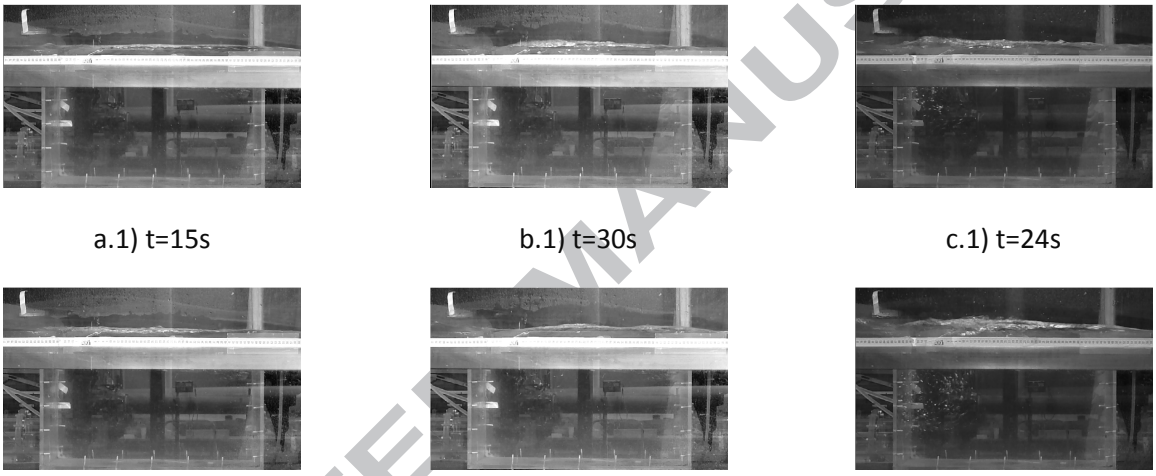

a.1) t=15s b.1) t=30s c.1) t=24s

a.2) t=21s b.2) t=9s c.2) t=15s

Fig. 10 Images of the air-water flow for reverse flow for 4(a), 5(b) and 6(c) l/s for two random instants in time.

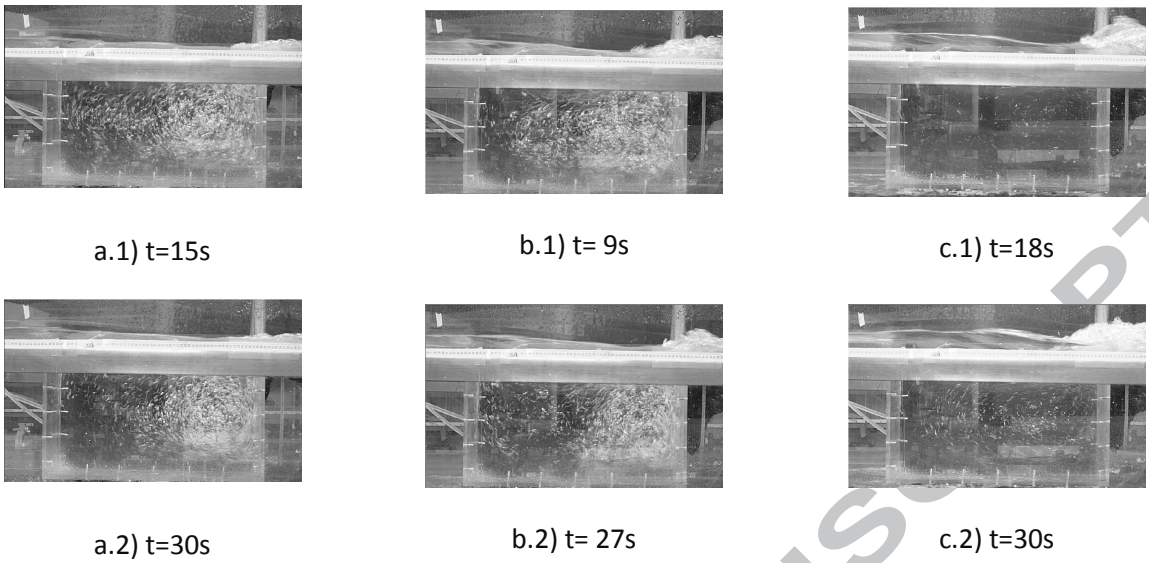

a.1) t=15s b.1) t= 9s c.1) t=18s

a.2) t=30s b.2) t= 27s c.2) t=30s

Fig. 11 Images of the air-water flow for drainage flow for 15(a), 22(b) and 32(c) l/s for two random instants in time.

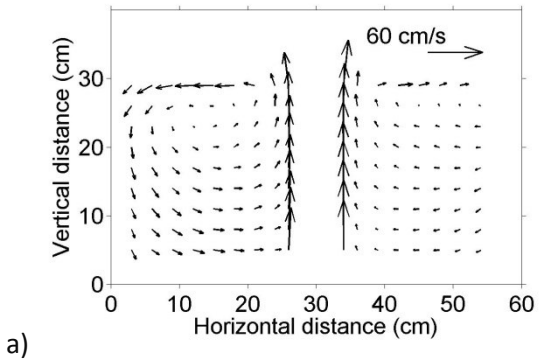

a)

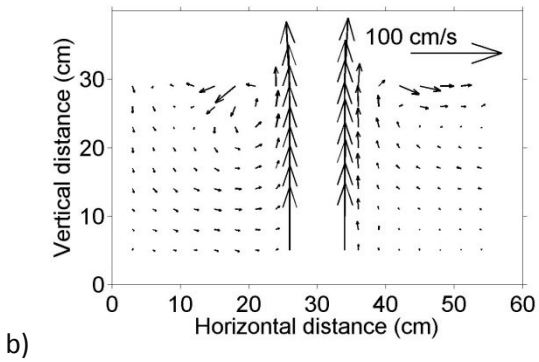

b)

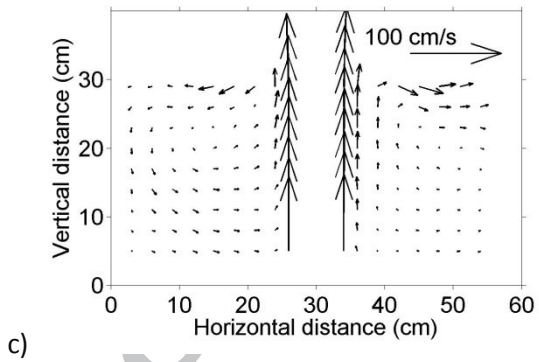

c)

Fig. 12 Average velocity vector field obtained with the numerical model for reverse flow for 4(a), 5(b) and 6(c) l/s.

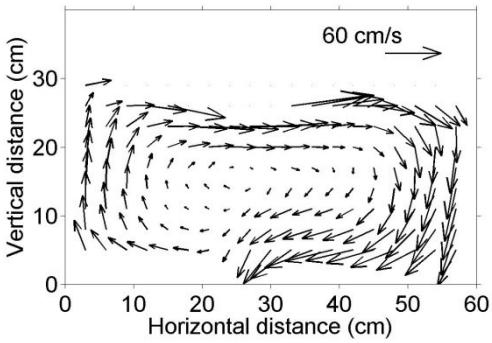

a)

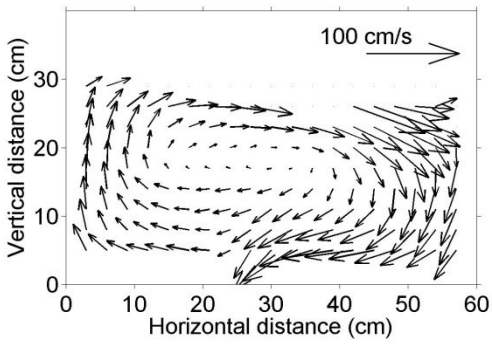

b)

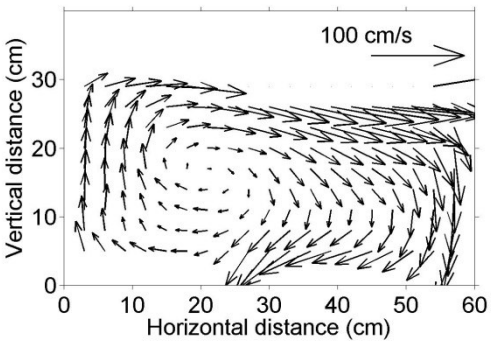

c)

Fig. 13 Average velocity vector field obtained with the numerical model for drainage flow for 15(a), 22(b) and 32(c) l/s.

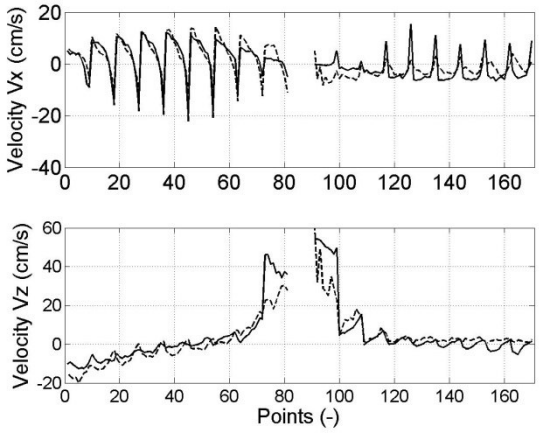

a)

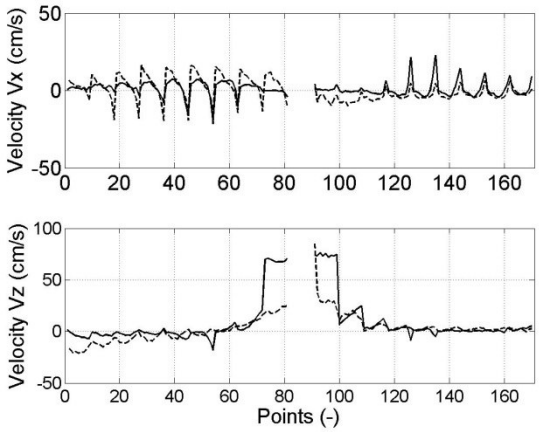

b)

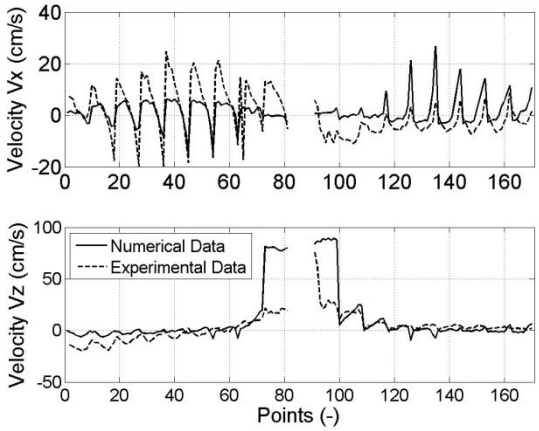

c)

Fig. 14 Comparison of the numerical and

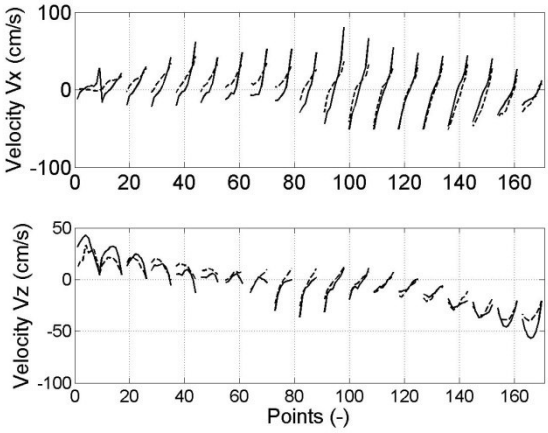

a)

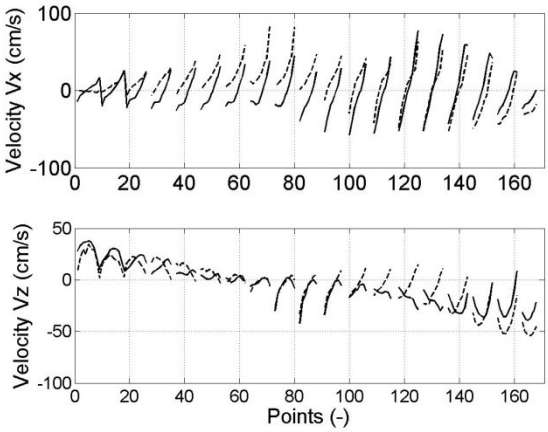

b)

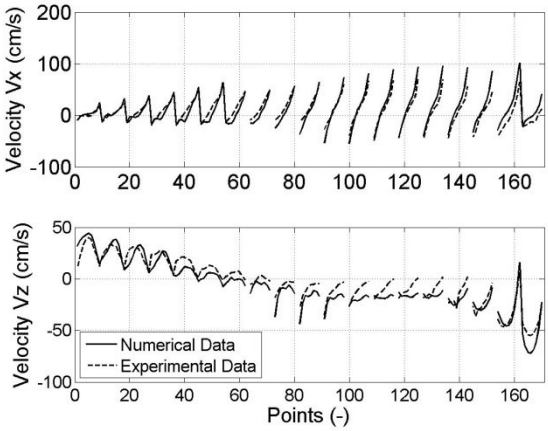

c)

Fig. 15 Comparison of the numerical and

experimental average velocity vector field for reverse flow for 4(a), 5(b) and 6(c) l/s.

experimental average velocity vector field for drainage flow for 15(a), 22(b) and 32(c) l/s.

Table 1 Summary of the flow conditions run in the MLE experimental installation for studying reverse (Tr) and drainage flow (Td).

Test ID	Q(l/s)	U(m/s)	H(m)	Fr	Re	Frequency (Hz)	Sampling Period (s)
Tr.1	4	0.80	0.760	0.90	$6x10^4$		
Tr.2	5	0.99	0.830	1.12	$8x10^4$	1	180
Tr.3	6	1.19	0.910	1.34	$10x10^4$		
Td.1	15	0.99	0.030	1.80	$8x10^4$		
Td.2	22	1.18	0.037	1.94	$9x10^4$	25	180
Td.3	32	1.36	0.047	2.00	$10x10^4$		

Table 2 Summary of the calibration results of the 4 l/s reverse (Tr) numerical model, including LES parameters (Cε, Ck), maximum velocity (Vmax) and average velocity fields at the left (Vavl) and the right (Vavr) side of the Gully, absolute errors, computational time (Time), and measures of Fit.

LES Parameters		Numerical Velocities (cm/s)			Abs Errors (cm/s)			Time	Measures of Fit		
Cε	**Ck**	**Vavl**	**Vavr**	**Vmax**	**Vavl**	**Vavr**	**Vmax**	**(s)**	**PBIAS**	**I.d**	**R^2**
0.93	0.0943	7.43	5.06	57.61	-2.88	0.08	-2.13	155416	-0.07	0.89	0.76
1.05	**0.03**	**10.18**	**6.43**	**54.50**	**-0.13**	**1.44**	**-5.24**	**95522**	**-0.15**	**0.90**	**0.85**
1.05	0.055	8.27	6.33	58.58	-2.04	1.35	-1.16	81845	-0.16	0.90	0.85
1.05	0.07	8.61	5.98	57.72	-1.70	0.99	-2.02	76547	-0.16	0.89	0.79
1.15	0.07	9.83	7.24	55.24	-0.48	2.25	-4.50	116063	-0.19	0.91	0.85
1.25	0.07	7.84	6.96	53.58	-2.48	1.97	-6.15	113671	-0.13	0.89	0.65
1.25	0.055	7.89	6.66	56.97	-2.42	1.67	-2.76	157704	-0.16	0.89	0.74
Experimental		10.31	4.99	59.74	--	--	--	--	--	--	--

Table 3 Summary of the calibration/validation results of the of the reverse (Tr) and drainage (Td) numerical model tests with corresponding measures of fit.

Test ID	Q (l/s)	Measures of Fit PBIAS	I.d	R^2
Tr.1 (c)	4	**-0.15**	**0.90**	**0.85**
Tr.2	5	-0.15	0.68	0.67
Tr.3	6	-0.15	0.60	0.62
Td.1	15	-0.16	0.90	0.85
Td.2	22	0.01	0.78	0.62
Td.3	32	-0.12	0.89	0.84

Note: (c) = calibration run.

Highlights

- We model experimentally and numerically a gully box.
- We simulate turbulence with LES Smagorinsky using the OpenFoam toolbox.
- Reverse flow shows strong jet at the centre and an anticlockwise vortex on the left side.
- Drainage flow shows a clockwise vortex above and to the left of the bottom outlet.
- Drainage flow exhibits large quantities of air-entrainment caused by a hydraulic jump.